SMAR 2019 – Fifth Conference on Smart Monitoring,
Assessment and Rehabilitation of Civil Structures

SMAR 2019

Optimization of frequency ranges in health monitoring of RC frame using embedded PZT sensors

Moinul HAQ [1], Tabassum NAQVI [1], Suresh BHALLA [2]

[1] Civil Engineering Department, Aligarh Muslim University, Aligarh, India

[2] Civil Engineering Department, Indian Institute of Technology, New Delhi, India

Contact e-mail: mmhaq2010@gmail.com

ABSTRACT: The present study experimentally investigates the systematic performance in monitoring the high cycle fatigue damages of Reinforced Concrete (RC) frame structure while implementing the Electro-mechanical Impedance (EMI) technique. PZT transducers embedded in concrete frame in form of ceramic patches has been excited electrically at healthy and damaged states of frame prototype for acquiring mechanical impedance based signature responses in different frequency ranges. For the purpose of optimization, seven different exciting frequencies ranges i.e. 100 kHz - 150 kHz, 150 kHz - 200 kHz, 100 kHz - 200 kHz, 500 kHz - 600 kHz, 600 kHz - 700 kHz, 900 kHz - 1000 kHz, and 20 Hz - 1000 kHz were chosen for obtaining reliable estimation of damage severity due to induced fatigue loads. Signatures variations in form of root mean square deviation (RMSD) and cross-coefficient damage metric (CCDM) for impedance real part, i.e. conductance (G) and as well as for imaginary part i.e. susceptance (B) in user defined frequency ranges has been plotted and compared for different damaged states. Results revealed a successful demonstration in predicting fatigue damage using embedded PZT sensors in frequency range 100 kHz - 200 kHz when compared with other considered frequency ranges. Findings of the present study guide the future researchers and engineers to take concise frequency ranges while monitoring the health of RC structures ultimately saving the procedure time while ensuring effectiveness of PZT transducers in arresting high cycle fatigue damages.

1. INTRODUCTION

The applications of smart materials have been categorised as the prominent and effective solutions to various problem in field of structural health monitoring (SHM) and energy harvesting. Piezoelectric materials are one of its kinds used in developing an interaction between structural mechanics and electricity. These types of materials are capable of generating electrical charges at nano- and micro-scale while got stressed with even at small magnitudes which opens their passage in sensing and energy harvesting based applications (Bhalla et al. 2017; Haq, Bhalla, and Naqvi 2017). Another key application is using it as actuating devices as stresses generation is also controlled by orienting material dipoles while passing the electric current through it. The uniqueness of these materials has put them in category of being smart or intelligent and opens various paths for researchers to explore & unfold efficient and precise health monitoring techniques and maximising energy output for making a sustainable environment. In past couple of decades Lead Zirconate Titanate (PZT) has been marked as the popular piezo materials for its utilisation as transducer. PZT in form of ceramics patches and nano films due to its more sensitiveness has been extensively used for detecting damages and

failures in civil structures as well as for living organs (Haq 2018). Particularly for piezoelectric materials based SHM, various theories such as fluctuating method, local and global dynamics techniques, mechanical impedance method, and vibration based techniques are popularly used. Different studies to verify the EMI techniques in damage detection and in estimation of structural health with precision have been demonstrated by various researchers around the globe. Bhalla and his research group have reported various experimental, analytical and numerical studies on effective health monitoring of structures using surface bonded as well as embedded PZT sensors. Wang et al. formulates the EMI technique based damage indices for finding the damage locations in a beam (Wang, Song, and Zhu 2013). The experimental results were validated with the numerical simulations with a good agreement between them. The concrete behaviour under fatigue loads follows two phases i.e. deceleration stage followed by acceleration stage till failure (Mu, Subramaniam, and Shah 2004). The theory was based on rate of change of the stiffness that defines crack initiation stage, crack propagation stage and failure stage with sudden loss of extensive stiffness relative to number of induced fatigue cycles. A study related to the present work has been recently reported in field of EMI that assessed fatigue damages in the concrete beams (Bhalla and Kaur 2018). The EMI technique has been proved beneficial in finding the real-time stiffness change response for the concrete structure and has proved its efficiency to find damage severity alternate to traditional time consuming *S-N* curve approach. However, the frequency ranges of electrical excitations in the study have been randomly considered in lower ranges as by reviewing the previous reported literature. Further, no concept for using a particular damage index that provides significant variations in visualising damages locations and severity in concrete had been discussed. The answers to these types of problems have been complemented in the present work.

The optimisation of the frequency ranges used in the EMI technique during fatigue monitoring of the RC frame structure have been carried out by performing an experiment. The PZT patch in embedded form operating in dual mode, i.e. both as sensor and actuator has been utilised for accessing electrical charge based output based on severity of fatigue damages. For the purpose of ascertaining maximum damage output, two different damage indices based on responses of real and imaginary admittance are quantified and compared for three different damaged states in different excitation frequencies.

2. EXPERIMENTAL PROGRAM

2.1. Specimen and Material characteristics

The present health monitoring experimental investigations have been conducted on a RC frame specimen having columns bottom fixed to the shake table. The dimension of the sections for beam and column has been chosen 0.12 m x 0.12 m and 0.12 m x 0.18 m respectively. The end-to-end height and width of the frame is 1.22 m and 1.45 m respectively having main reinforcement comprising 4 bars of 12mm diameter and shear reinforcement of 6 mm bars at 120 mm c/c spacing. The minimum criteria for the flexure and shear reinforcement have been satisfied by estimating using Indian code limit state design provisions stated in IS 456 (Indian Standards 2000). The grade of the concrete and steel reinforcement has been constrained to M20 and Fe415 respectively. The PZT transducer in form of ready-to-use packed cement composite, known as Concrete Vibration Sensor (CVS) has been embedded at position of beam-column joint in the frame. This location is chosen so as to induce maximum sensitiveness to embedded strain-based PZT sensor. Figure 1 show the reinforced concrete frame clamped to the shake table studied for monitoring damages induced due to fully reversed cyclic loads.

The piezoelectric ceramic square shaped patch PZT-5H model in embedded form was used to monitor the health of the concrete structure. The dimension of PZT patch is 10mm x 10mm x 0.2mm procured from central electronic limited, New Delhi, India in form of cylindrical shaped CVS having diameter 25mm and thickness of 10mm. The CVS are embedded in concrete so as to perform PZT patch operations under d31 mode which symbolize charge generation along PZT thickness transverse to stress induced to patch. The relation governing the piezoelectricity law in PZT patches is given in equations (1) and (2).

$$D_3 = \varepsilon_{33}^{T} E_3 + d_{31} T_1 \quad (1)$$

$$S_1 = T_1 Y^E + d_{31} E_3 \quad (2)$$

where S_1 and D_3 are the strain in direction '1'and electric displacement or say charge density in PZT patch respectively, d_{31} , E_3 and T1 are the piezo electric strain coefficient, external electric field and axial stress in direction '1' respectively. Y^E and ε^T_{33} are the complex elastic modulus of the PZT patch at constant electric field and complex electric permittivity in direction '3'at constant stress respectively. Eqn. (1) is employed in sensing applications, whereas Eqn. (2) for actuation purposes.

Mechanical and electrical properties of considered PZT-5H patch have been written in Table 1.The sinusoidal cyclic load is induced using shake table with an acceleration of intensity of 0.3g meter per square seconds from the bottom of columns. The testing temperature during the experiment has been adhered to 20˚ ± 4˚C for minimizing the error due temperature gradient. Another importance has been given in providing maximum fixity of frame structure to the shake table top while welding the 12mm thick steel plates from column sides and reinforcement with shake table. More details related to CVS and PZT has been found in previously reported researches (Dixit and Bhalla 2018; Haq et al. 2017; Kaur and Bhalla 2014).

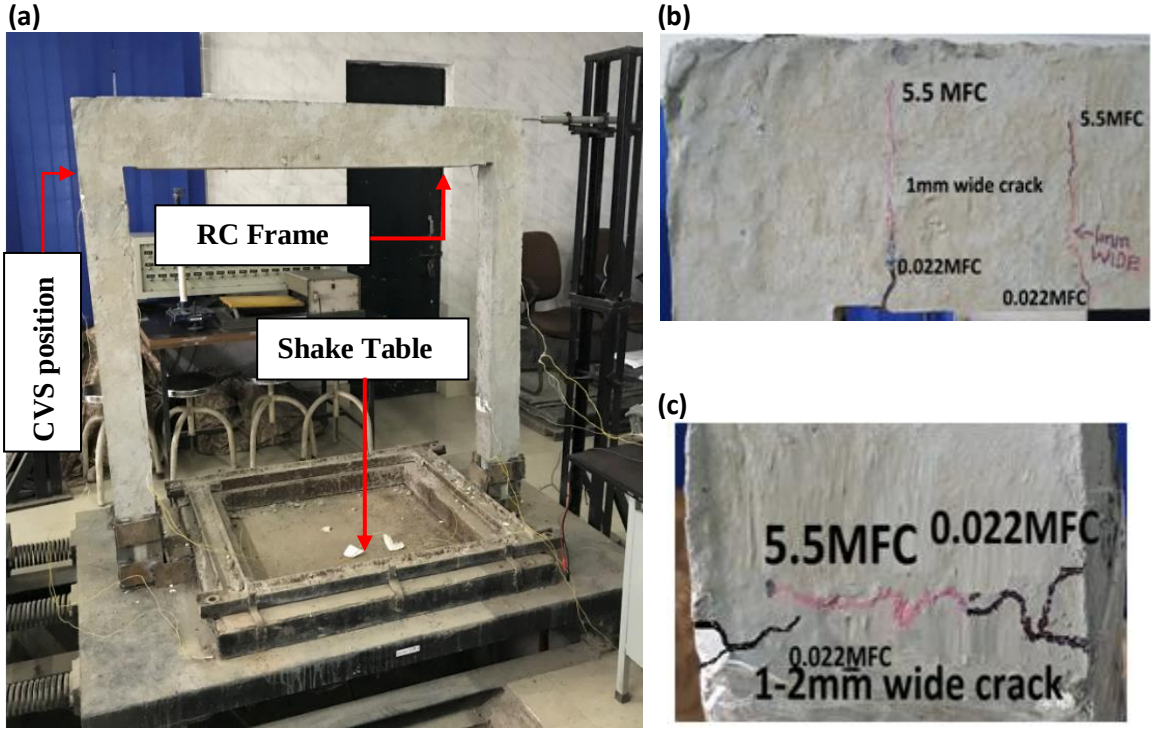

Figure 1. (a) Typical setup of healthy reinforced concrete frame clamped on shake table; (b) Cracks developed in beam of considered RC frame near CVS location after failure; and (c) Cracks developed in column of RC frame near CVS location after failure.

Table 1: Characteristics of PZT-5H patch considered for SHM (Peizoelectric Ceramics 2018).

Property	**Value**
Young's modulus (Y^{E}_{11})	6.667 x 10^{10} MPa
Loss Tangent	0.0224
Density	7.4 gm/cc
Mech. Q	70
Dielectric Constant at 1 KHz	3250
Coupling co-efficient	
K_P	0.56
K_{31}	0.34
K_{33}	0.68
Piezoelectric Charge constant (x10^{-12}), D_{33}	580 C/N
Piezoelectric Voltage constant (10^{-3}), g_{33}	20 Volts-meter/ Newton

2.2. Philosophies involved in PZT sensor based SHM

Global dynamics (GD) and Electro-mechanical impedance (EMI) technique are the two methodologies involves traditionally in field of electrical based health monitoring (Kaur and Bhalla 2014; Mazlina et al. 2015). GD technique involves in acquiring the physical response of the system under critical loading environment. Modes shapes are build-up for different damage states and compared later to access the structural health. On the other side, EMI technique involves study of piezo-structure interaction that involves actuating the PZT patch electrically and acquiring the response from the same PZT while exciting it electrically in user-defined frequency ranges. It has been observed from literature that PZT identified parameters differs with characteristics of PZT patch and host materials. Further change in excitation frequencies affects the electro-mechanical impedance of the structure. The present study has been carried out for the purpose of optimising these frequency ranges so as to implement the EMI technique more efficiently for reinforced concrete structures.

3. OBSERVATIONS

In the present experiment the PZT patch is designed to work under dual mode operation i.e. both for sensing as well as for actuating the host. Electromechanical impedance technique has been adopted to acquire the impedance response of the RC specimen during its entire fatigue life. The admittance as the inverse of impedance is hereby observed within the user-defined frequency range using LCR meter. Mathematical relation for electrical admittance was given by Bhalla given in equation 3 (Bhalla et al. 2017; Moharana and Bhalla 2014).

$$\bar{Y} = G + jB = 4\omega \frac{l^2}{h}\left\{\overline{\varepsilon_{33}^{T}} - \frac{2\overline{Y^{E}}d_{31}^{2}}{1-\upsilon}\left(\frac{Z_{a,eff}}{Z_{s,eff}+Z_{a,eff}}\right)\frac{\tan Ckl}{Ckl}\right\} \quad (3)$$

Where, 'ω' is angular frequency, 'υ' is poison's ratio, 'l' and 'h' be the width and thickness of PZT patch, 'C' is correction factor, 'κ' is the wave number and $\overline{Y^{E}}$ be the complex young's modulus of PZT patch. As shown in mathematical relation, the admittance comprises a real part termed as conductance represented by a symbol 'G' and an imaginary part susceptance represented by a symbol 'B', whose data is recorded in prolong frequency range in between 20 kHz to 1 MHz at sampling interval of 1 kHz. The data is recorded for three states of damages, first for the pristine or say healthy state, second for initial phase of fatigue life after 22000 load cycles or say 0.022 million fatigue cycles (MFC), and third lastly as failure state after 5.5 MFC. Figure 2 (a) and Figure 2(b) shows the variation of conductance (G) and susceptance (B) signatures at the taken three damage states in the entire fatigue life.

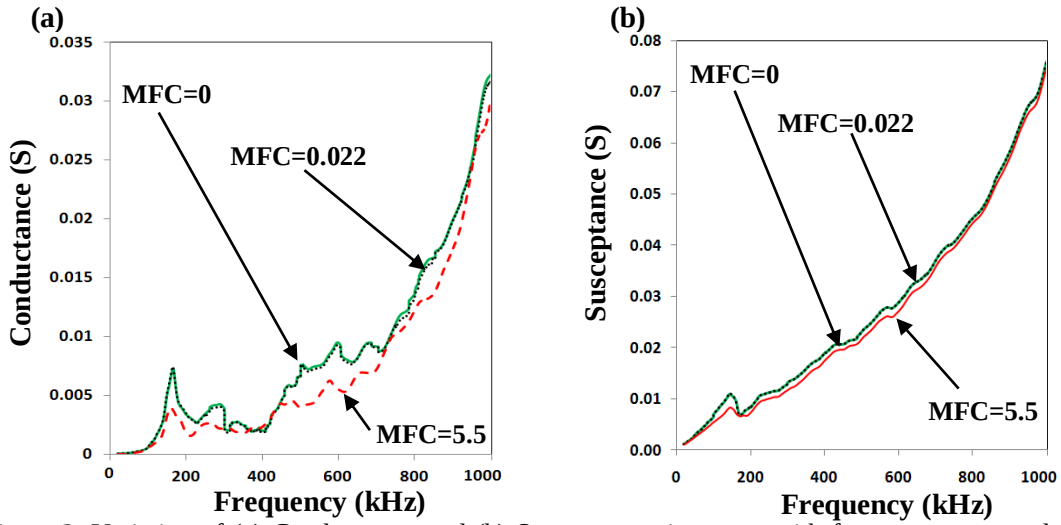

Figure 2. Variation of (a) Conductance, and (b) Susceptance signatures with frequency measured using embedded PZT transducer (Range: 20 kHz – 1000 kHz).

A lower and left shifting of peaks for both real and imaginary part of admittance signatures has been observed with increasing fatigue damage in RC frame. This structural-PZT interaction will enable the user in quantifying the health at any damage state while analysing these signatures pattern. The lowering of G and B peaks has a little variation in the initials load cycles stages that verifies the little stiffness loss in fatigue stage-I as given by Mu at al. (Mu et al. 2004). The loss in G and B values maximised as due to sudden failure after loading cycles reaches 5.5 million counts during the fatigue stage-III. It has been observed that the variation of significant variation in admittance values pertain in only few frequency ranges at different intervals. The shifting of *G* and *B* peaks depends on the properties of host, PZT patch and bonding along with the excitation frequency range. A correct frequency ranges will enable the user to monitor the health of structure effectively by analysing these variations of peaks and consecutively helps in precise estimation of remaining life. The main focus while analysing the signatures is given in optimising the frequency range to get maximum stimuli output rather than to validate the damage pattern in lieu of induced fatigue damages.

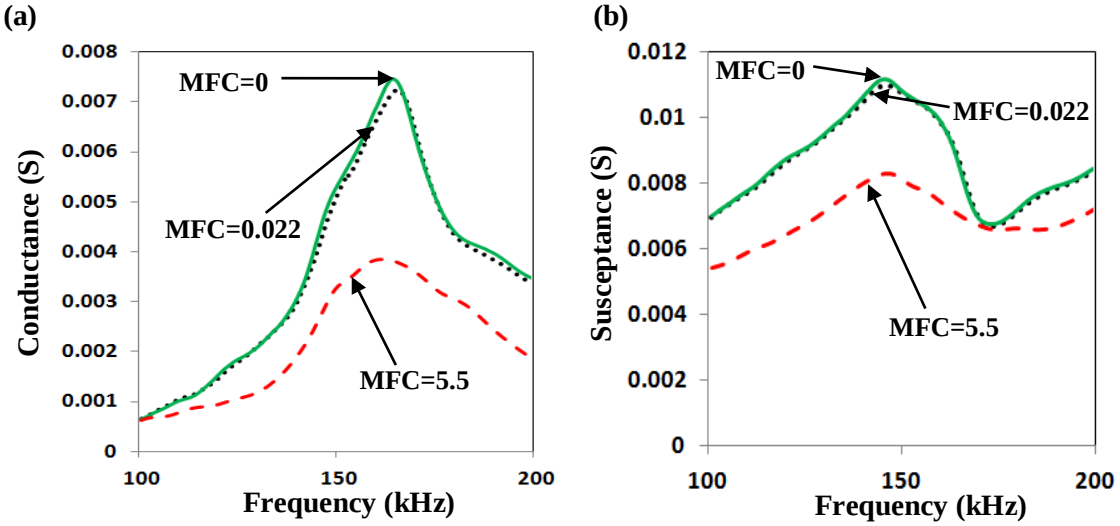

Figure 3. Variation of (a) Conductance, and (b) Susceptance signatures with frequency measured using embedded PZT transducer (Range: 100 kHz – 200 kHz).

To optimize the results, the *G* and *B* signatures are visualised deeply at different frequency ranges such as 100 kHz – 150 kHz, 150 kHz – 200 kHz, 100 kHz – 200 kHz, 500 kHz – 600 kHz, 600 kHz – 700 kHz, 900 kHz – 1000 kHz, and 20 kHz – 1MHz. Figure 3 shows the magnified image of real and imaginary admittances variations for different damage states in excitation frequency between 100 kHz- 200 kHz. It has been noticed that maximum shifting of admittance signatures is attained at peaks ranges in lower frequency ranges when compared with that of higher sides. Mathematical analysis has been worked out to quantify these variations in terms of magnitudes discussed briefly in next section.

4. RESULTS

The health monitoring of the structure is conventionally accessed by using statistical formulation evaluating the changes in observed electrical bound parameters with respect to failures induced during its entire life. In the present study, damage assessment has been demonstrated by using two types of damage indices, namely root mean square deviation (RMSD) and correlation coefficient damage metric (CCDM), based upon the changes in conductance and susceptance signatures in various user defined excitation frequency ranges. These indices ultimately helps in accessing the health of structure and are proved effective in localizing damage and estimating damage severity. The expression for quantifying RSMD index for PZT identified admittance is shown in equation (4) (Naidu and Bhalla 2002).

$$RMSD(\%) = \sqrt{\frac{\sum_{i=1}^{N}(Y_i^1 - Y_i^0)^2}{\sum_{i=1}^{N}(Y_i^0)^2}} \times 100 \quad (4)$$

Where Y_i^1 and Y_i^0 represents the post and pre-damage value for real and imaginary admittance at i^{th} data point. A plot for RMSD index, in percentage change, for conductance variations and susceptance variation is shown in Figure 4(a) and Figure 4(b) respectively for frequency ranges given in previous sections. The frequency ranges are chosen by visualizing the *'G'* and *'B'* peaks in Figure 2 and Figure 3 for estimating maximum possible variations.

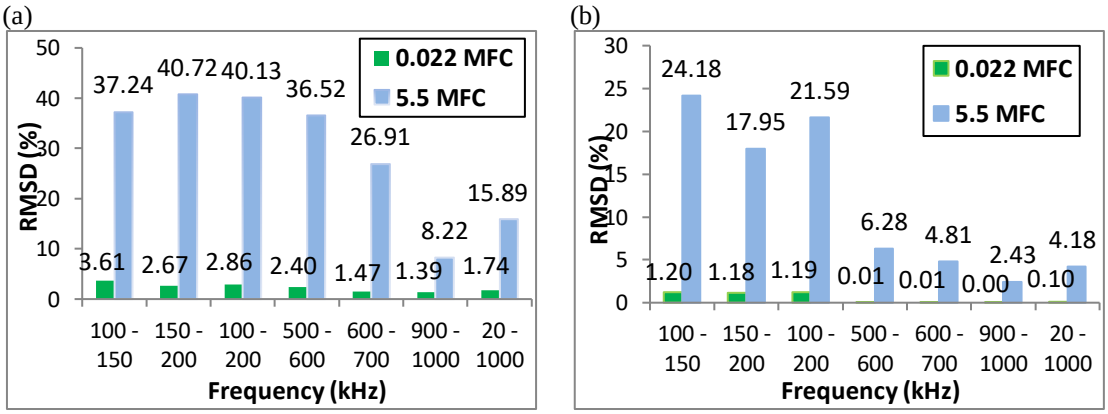

Figure 4. RMSD variations for (a) Conductance, and (b) Susceptance signatures relative to different excitation frequency ranges considered for PZT transducer.

While analyzing RMSD plots for '*G'* and '*B'* signatures shown in Figure 4(a & b) it was found that value of index increases with increasing fatigue damage in the RC frame. It was also observed that maximum deviation occurs in lower frequency ranges of about 100 kHz – 200 kHz relative to higher frequency ranges. The change in RMSD value for conductance is higher in 150 kHz – 200 kHz ranges whereas 100 kHz - 150 kHz frequency range shows higher

variation of RMSD based on susceptance variation. Overall a good and acceptable RMSD variation in lower frequency range of 100 kHz - 200 kHz for both the conductance and susceptance signatures was observed for estimating the concrete fatigue damage. On the other hand a descending variation of RMSD index has been observed while working with higher excitation frequencies. Further, RMSD index values for conductance signatures were observed higher than corresponding values for susceptance signature that proved more effectiveness and higher sensitivity of using conductance signature variation rather than susceptance for estimation of fatigue damages developed in concrete structure during its life span.

Another conventional damage index in field of health monitoring that is quite used for estimating damage in concrete and steel structures is correlation coefficient damage metric (CCDM). The mathematical relations evaluating CCDM, in percentage, is written in equation (5), (6) and (7) (Hu, Zhu, and Wang 2014; Wang et al. 2013).

$$Covariance = \frac{1}{N}\sum_{i=1}^{N}\left(Y_i^1 - \overline{Y^1}\right)\left(Y_i^0 - \overline{Y^0}\right) \quad (5); \qquad CC = \frac{Covariance(Y_i^1, Y_i^0)}{\sigma_{Y^1} \times \sigma_{Y^0}} \quad (6)$$

$$CCDM(\%) = (1 - CC) \times 100 \quad (7)$$

Where, Y_i^1 and Y_i^0 represents the post and pre-damage value for real and imaginary admittance at i^{th} data point, $\overline{Y^1}$ and $\overline{Y^0}$, represents averaged value for post and pre-damage real and imaginary admittance in user defined frequency and '*CC'* be the correlation coefficient. A plot for CCDM index, in percentage change, for conductance variations and susceptance variation is shown in Figure 5(a) and Figure 5(b) respectively for same frequency ranges as taken for quantifying RMSD given in previous section. The values of CCDM index has been found increasing at 5.5 million induced fatigue cycles (MFC) with respect to 0.022 million fatigue cycles for all the ranges of frequencies considered in analysis. From the shown index plots it is also observed that maximum variation for CCDM values for conductance signatures is occurred in frequency range of 150 kHz - 200 kHz whereas 100 kHz - 200 kHz frequency range represent higher CCDM variation for susceptance signature upon fatigue damage. Although, similar to RMSD, again an acceptable variation in CCDM value has been observed in 100 kHz – 200 kHz frequency for both '*G'* and '*B'* signatures against concrete fatigue damage. Similar to RMSD plots, lower CCDM index value has been observed while exciting PZT patch in higher frequency as shown in Figure 5. However, contrary to RMSD plot, higher CCDM index values were observed for susceptance in frequency 100 kHz-200 kHz relative to variations in conductance signature.

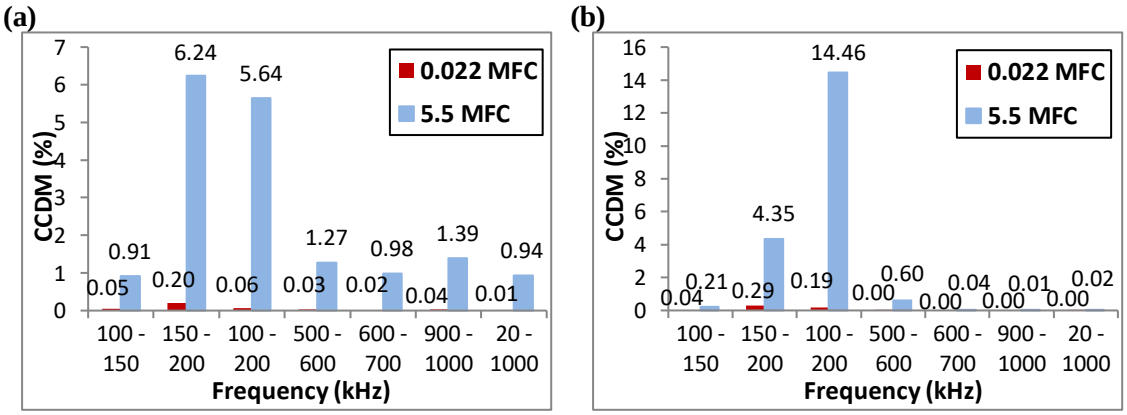

Figure 5. CCDM variations for (a) Conductance, and (b) Susceptance signatures relative to different excitation frequency ranges considered for PZT transducer.

5. CONCLUSIONS

The experimental demonstration of utilizing EMI technique during monitoring high cycles fatigue damages in RC frame has been carried out successfully. Both the conductance and susceptance signatures acquired using embedded PZT patch in defined frequency ranges observed the lower-left shifting of peaks values with increasing fatigue cycles. This shifting in output signatures has been quantified and compared using two different statistical damage indices i.e. RMSD and CCDM. During EMI based SHM, it has been shown, that the damage indices variations has attain maximum values when PZT patch was excited in lower frequency range when compared to higher ones. A frequency range of 100 kHz - 200 kHz have been found satisfactory in providing the high variations of damage indices. Moreover the RMSD index plotted for conductance variations has shown more tendencies in ascertaining high cycle fatigue damages of concrete. From the present study, it has been recommended to use conductance based signatures in lower frequency while implementing EMI technique on RC structures. This would be helpful in obtaining more sensitiveness of PZT patch towards the damages ultimately saves the user times in performing tedious experimental and analytical work. The future work may include proving the effectiveness of embedded PZT sensors in assessing the strength and stiffness loss, load sustainability consecutively ascertaining the residual life of the RC structure.

6. ACKNOWLEDGEMENT

First author acknowledged the Senior Research Fellow (SRF) financial assistance (Letter No. 09/112(580) 2k18) from Council of Scientific and Industrial Research, New Delhi, India during present investigations.

7. REFERENCES

Bhalla, S., S. Moharana, N. Kaur, and V. Talakokula. 2017. *Piezoelectric Materials: Applications in SHM, Energy Harvesting and Biomechanics*. John Wiley & Sons.

Bhalla, S. and N. Kaur. 2018. "Prognosis of Low-Strain Fatigue Induced Damage in Reinforced Concrete Structures Using Embedded Piezo-Transducers." *International Journal of Fatigue* 113:98–112.

Dixit, A. and S. Bhalla. 2018. "Prognosis of Fatigue and Impact Induced Damage in Concrete Using Embedded Piezo-Transducers." *Sensors and Actuators, A: Physical* 274:116–31.

Haq, Moin Ul, S. Bhalla, and Tabassum Naqvi. 2017. "Fatigue Damage Assessment of RC Column Using PZT Sensors." *Procedia Engineering*. Vol. 173:1223–30

Haq, Moinul. 2018. "Application of Piezo Transducers in Biomedical Science for Health Monitoring and Energy Harvesting Problems." *Materials Research Express* 6(2):022002.

Hu, Xianyan, Hongping Zhu, and Dansheng Wang. 2014. "A Study of Concrete Slab Damage Detection Based on the Electromechanical Impedance Method." *Sensors (Switzerland)*.

Indian Standards.2000.*IS-456:2000-Plain and Reinforced Concrete – Code of Practice (Fourth Revision)*.

Kaur, N. and S. Bhalla. 2014. "Combined Energy Harvesting and Structural Health Monitoring Potential of Embedded Piezo Concrete Vibration Sensors."*Journal of Energy Engineering* 141(91):1–58.

Mazlina, M. H. et al. 2015. "Bone-Crack Detection by Piezoeletric-Electromechanical Impedance Method." *International Conf. on Computer, Communication, and Control Technology*. Pp. 418–21

Moharana, S. and S. Bhalla. 2014. "A Continuum Based Modelling Approach for Adhesively Bonded Piezo-Transducers for EMI Technique." *International Journal of Solids and Structures*.

Mu, B., KV Subramaniam, and SP Shah. 2004. "Failure Mechanism of Concrete under Fatigue Compressive Load." *Journal of Materials in Civil …* 16(6):566–72.

Naidu, A. S. K. and S. Bhalla. 2002. "Damage Detection in Concrete Structures with Smart Piezoceramic Transducers." in *Smart Materials, Structures, and Systems*, Vol. 5062:684–90.

Peizoelectric Ceramics.2018."ProductCatalogue."*CentralElectronics Limited*.(http://www.celindia.co.in/)

Wang, D., H. Song, and H. Zhu. 2013. "Numerical and Experimental Studies on Damage Detection of a Concrete Beam Based on PZT Admittances and Correlation Coefficient." *Construction and Building Materials* 49:564–74.